Radiographic sensitivity improved by optimized high resolution X -ray detector design.

Lars Hammar, Håkan Wirdelius

Department of Materials and Manufacturing Technology
Chalmers University of Technology
SE-402 72 Göteborg, Sweden
Phone: +46 (0)31 7722692, Fax +46 (0)31 7724879
lars.hammar@chalmers.se, hakan.wirdelius@chalmers.se

Abstract
A compact imaging detector, based on scintillation fiber optics, has been used for high resolution industrial radiography since 1996. This type of imaging detectors have proven to give superior performance compared to fine grained industrial x-ray film in terms of detection efficiency and spatial resolution.
The objective of this paper is to show that the radiographic sensitivity can be improved even further.
First, the detection process has been studied by Monte-Carlo simulations and the result shows that the radiation is detected in a very narrow range from the axis of the primary beam.
Secondary, Monte-Carlo simulations shows that a bent fiber optic image conduit can eliminate radiation induced noise in the CCD almost completely and reduce the depth of the detector to less then 100 mm.
Keywords: Digital radiography, fiber optic scintillator, crack detection, nuclear

1. Introduction

Scintillation fiber optic faceplates were introduced as x-ray imaging detectors more then a decade ago [1]. Experiences from first generation imaging detectors based upon scintillation fiber optics (SFO) have been very promising, especially for high energy x-ray radiography. The objective of this paper was to quantify the essential parameters for optimizing the radiographic sensitivity in X-ray imaging detectors used for high energy industrial radiography. In this article is high energy radiography defined as industrial radiography on object similar to 30 mm steel and X-ray energy > 300 kV. The technique is developed to reach higher image quality than with conventional film radiography.
The aim with this article is to present a model for optimization on radiographic sensitivity of an x-ray imager. As already mentioned SFO-based detectors have proven to be superior for use with high energy x-rays, but a conventional scintillating, CsI, will also be analyzed to get a quantitative comparison.
The photon/electron transport in the scintillating screens is simulated to calculate detection efficiency and spatial resolution in order to validate what is theoretically achievable.
The radiation induced noise is also simulated. Thus the direct hits of primary x-rays to the CCD can be minimized. The information from the simulation will be the bases for the manufacturing of the detector.

2. Background

Since 1996 a first prototype based upon scintillating glass fiber optic has been used [2]. It is an x-ray imaging detector with a cooled, full frame CCD together with a straight fiber optic image conduit used instead of a conventional lens (see Figure 1). The detection screen is a terbium activated glass fiber optic scintillating faceplate with a thickness of 10 mm. The idea behind this design was to achieve higher radiographic sensitivity than available with fine grained industrial x-ray film.

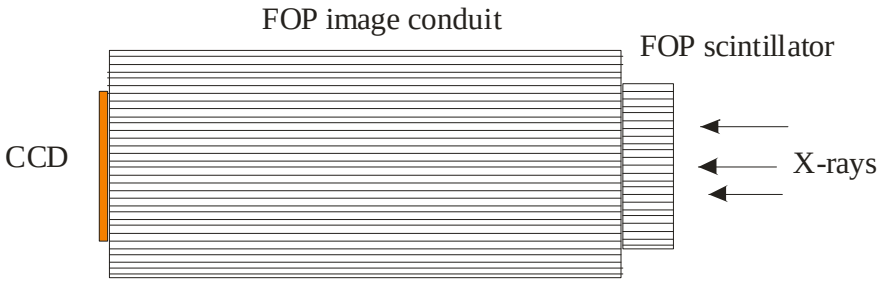

Figure 1. First generation fiber optic x-ray camera.

3. System overview

The system is designed for higher energies and is therefore based on the principle of indirect detection of x-rays. The x-rays are converted to visible light which are detected by a CCD and then converted to electrical signal. In the end the signal is digitized. This article is aimed to the main parts of the x-ray detection system which are the x-ray conversion screen, the lens system and the CCD unit. To get a clear view of the demands of the system it is important to shortly describe the whole chain, from the x-ray source to the x-ray image.

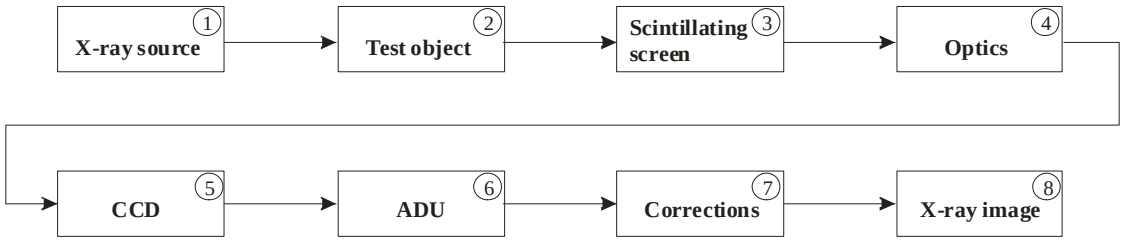

Figure 2. System overview.

The x-ray source creates the primary x-ray beam. As we are trying to optimize the system for objects with thickness in the range from 30 – 60 mm equivalent to steel the x-ray source (1) has to be a 450 kV machine.
The system was originally designed to detect, characterize and size service induced cracks in nuclear power plants. A typically test object (2) for this system is a thick

welded component in stainless steel or a nickel based alloy in the range of 30–60 mm in thickness. To be able to characterize such a crack the system should resolve very fine details.
The primary x-ray photons are detected and converted to visible light when they are attenuated or absorbed by the scintillating screen (3). The properties of the scintillating screen are very important and will be analyzed further in this article.
The optics or the lens (4) is guiding the light from the scintillating screen to the CCD. The demands on the optics are that it should be compact and guide the light efficiently and with as little aberrations and distortion as possible.
The CCD (5) converts the visible light to charges when the light photons are absorbed. The pixel size and the well capacity are important factors when choosing the CCD. It must be cooled below -30°C to enable exposures up to several minutes.
The collected charge from each pixel is digitized (6) by the analog-to-digital unit (ADU). Our present system is digitizing to 12-bit accuracy. A 16-bit format is available but 14-bit is enough as will be showed later.
The final image is affected by non-linearity in the optics and structural noise in the scintillating screen. The geometrical distortion arises from the drawing process and can be removed successfully by bi-linear transformation. The structural noise can easily be removed with background correction (7).

4. Energy deposition

The aim with the first simulation is to find the maximum achievable spatial resolution by estimating the (radiological) modulation transfer function of the energy deposition from the absorption of photons and secondary electrons. When the x-ray photons are absorbed, secondary electrons are produced according to the Compton- or the photo-electric effect. As the secondary electrons in the scintillating material slow down, atoms are ionized and produce the scintillating light when the atoms de-excite. The range of the secondary electrons depends on the electron energy and the density of the material. In this simulation, an infinite thin radiation beam along the central axis is used to simulate an (radiological) impulse response. This simulation will give data to estimate the minimum useful pixel size. In this simulation an infinite thin x-ray beam is filtered by a 50 mm thick object of steel (see Figure 3). The X-ray beam spectrum is simulated to be equivalent to a 450 kV x-ray machine (MGC 451). The purpose to put an object in the beam between the source and the detector is to get a true spectrum, including all secondary radiation effects.

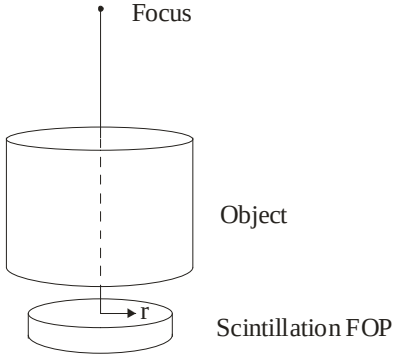

Figure 3. Monte-Carlo simulation of energy deposition.

Two types of scintillating faceplates are simulated. One is a 10 mm thick scintillating fiber optic glass and the other with 300 µm CsI(Tl). Only the result from the simulation of the fiber optic scintillating screen is presented here since they were almost identical. It shows that the MTF-curve drops to 10% at a distance of only 4 µm for both of them (see Figure 4). It means that most of the energy is detected inside a circle with diameter of 8 µm. This result corresponds well with earlier studies [3].

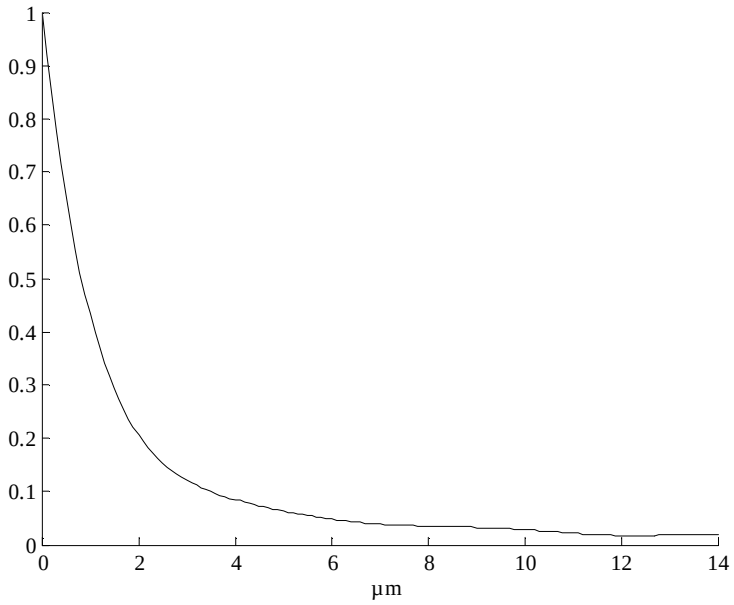

Figure 4. Energy deposition vs. radial distance.

5. Pulse height spectrum

Before we can calculate the detection efficiency we have to calculate the pulse height spectrum. As the majority of the primary photons are attenuated by the Compton-effect the deposited energy is only a fraction of the incoming energy. The energy of the detected x-rays is not uniform but distributed according to some probability distribution. The

effect of these fluctuation in light output can be expressed as an information transfer factor [4], I :

$$I = \frac{M_1^2}{M_2 \cdot M_0} \tag{1}$$

Where M_r is the r^{th} moment of the distribution (see Figure 5).

The simulation is done in a similar way as when the energy deposition was simulated. A 450 kV x-ray beam filtered by an 50 mm steel object was detected by an 11 μm fiber with a length of 10 mm. The value of I is 0.65 for this distribution which corresponds to earlier studies.

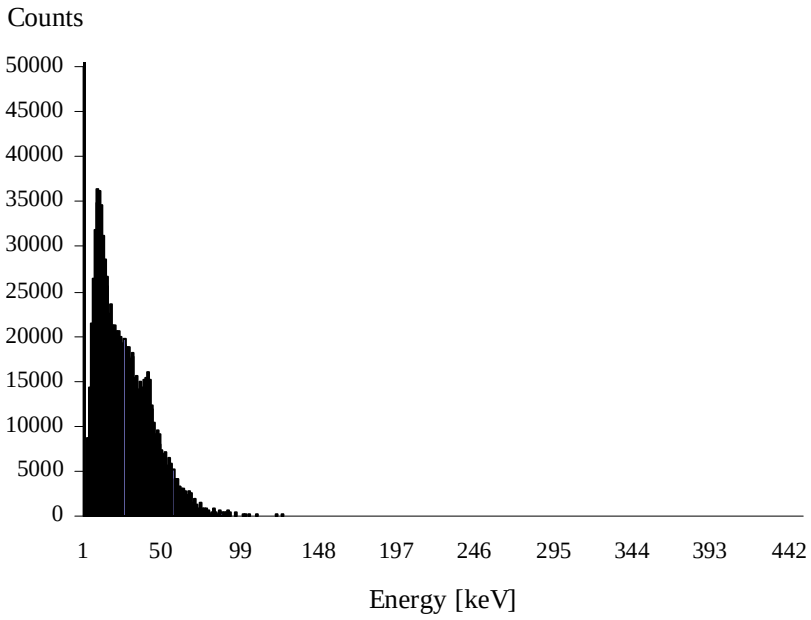

Figure 5. Pulse height spectrum for an 11 micron fiber.

6. Detection efficiency

A scintillation based x-ray detector produce light photons in the end of the optical chain, but it is the detected primary photons that creates an x-ray image. The statistics of an x-ray source follows the Poisson statistics. As the number of detected photons is large the Poisson can be replaced by the normal distribution. In order to achieve highest possible image quality, as many primary x-ray photons as possible should be detected in each pixel during an exposure. By practical reasons there is always a trade-off between available exposure time and image quality. A traditional detector (e.g. x-ray film) is limited by a maximum dose before it is overexposed. The maximum exposure times with electronic detectors such as x-ray image intensifier tubes and flat panels are usually less then 10 second due to thermal noise. The thermal noise can be reduced to a minimum by

using a Peltier cold CCD. To minimize the statistical noise we can accept long exposures and therefore choose a clock frequency to achieve low read-out noise. Ideally, the only significant noise source will then be the statistical noise.

The absorption efficiency, T_a, is defined as:

$$T_a = \textit{absorbed energy / incident photon energy} \tag{2}$$

The numbers of photon interactions per pixel governs the resulting signal-to-noise ratio (SNR). The SNR for an X-ray detector is:

$$SNR = \sqrt{T_a \cdot N \cdot I} \tag{3}$$

N is the number of X-ray photons impinging the scintillating phosphor screen and I is the information transfer function. To increase SNR, with given amount x-ray photons (N), T_a has to be increased. In traditional phosphor screens the thickness is decreased to improve the spatial resolution; which yields a low T_a and consequently a reduced SNR. Therefore, there was a tradeoff between spatial resolution and T_a.
The detection efficiency is poor for the radiographic film compared to phosphor screens which usually contains materials with high atomic number. X-ray detectors based on indirect detection have a scintillating phosphor screen as primary detection medium. The principal difficulty is to achieve high spatial resolution while maintaining high absorption efficiency. Thick phosphor screens yields poor spatial resolution due to lateral diffusion as the generated light is scattered isotropic at the point of scintillation.

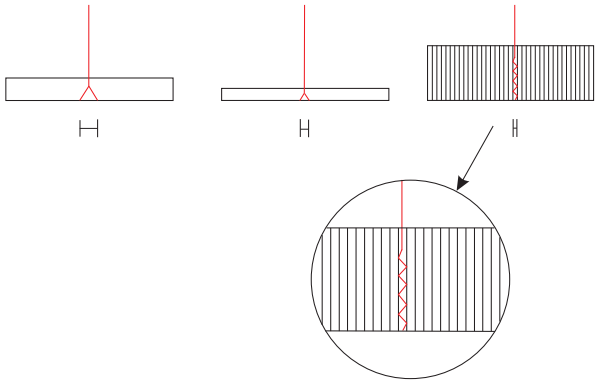

Figure 6. Conventional phosphors compared to fiber optic scintillators.

One way to overcome this problem is to use structured screens that can guide the generated light without lateral diffusion [1]. We will analyze two ways to achieve these properties; structurally grown CsI or fused fiber optic faceplates (FOS) made of scintillating glass. These solutions are able to guide the light inside the crystals or the

fibers by total internal reflection and thus be much thicker then traditional phosphor screens without loosing spatial information. The thickness of structurally grown CsI is typically 300 µm but the thickness can be up to 700 µm [5] and the FOS can be thicker then 10 mm. As the detector is optimized for higher energies, the emitted spectrum from the x-ray machine has to be filtered by an object before it is attenuated by the scintillating screen to compensate for the beam-hardening effect. All photons with low energy are absorbed by the object. The filtered spectrum is then divided into narrow bins (10 keV) and the attenuation coefficients for each bin are used to get the attenuation spectrum (see Figure 7). The upper curve is the filtered spectrum and the other three are FOS-, CsI-screen and Gadox-screen. The FOS-screen is 10 mm, CsI-screen is 300 µm and the Gadox-screen is 100 µm thick. The detection efficiency is about 37% for the mean energy for the SFO-screen while it is 3% for the CsI-screen and only 0.8% for the Gadox-screen. The light yield from a FOS-screen is low and usually considered as a drawback. Next section will show that it actually an advantage.

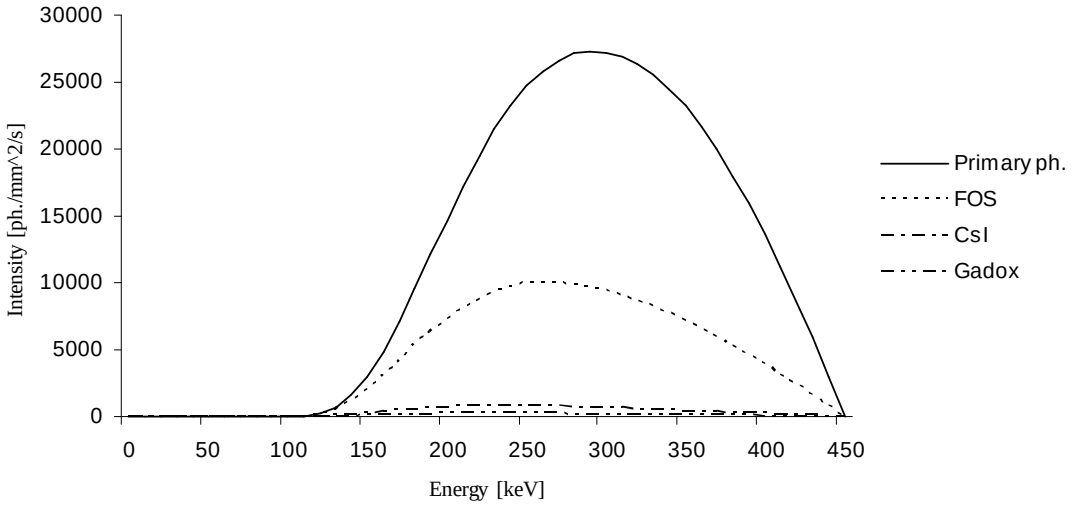

Figure 7. Filtered spectrum and attenuated radiation.

7. Detection quantum efficiency

To model the DQE, we normally need expressions for the whole chain of components specifying how the detected signal propagates through the detector. As there is no intensifying stage in the proposed detector, no additional noise sources have to be considered and therefore the model for calculating DQE of the phosphor itself can be used for the whole chain. DQE [6] for the detector is then given by

$$DQE = T_a /(1+ g^{-1}) \tag{4}$$

where, T_a, is the fraction attenuated by the phosphor and g, is the mean number of produced electrons (e^-) in the CCD for each attenuated, primary x-ray. Figure 8 shows the

relationship between DQE (left axis) and the number of e^-/x-ray detected by the CCD. Already at levels of conversion efficiency as low as 4-5 e^-/x-ray, DQE exceeds 80%. The CCD will be saturated before sufficient dynamic resolution is achieved if the conversion efficiency is considerably higher than 10 e^-/x-ray. The dynamic range is also plotted (right axis) in Figure 8. The light yield has to be maximized to a value around 10-20 e^-/x-ray to achieve a 14-bits dynamic range.

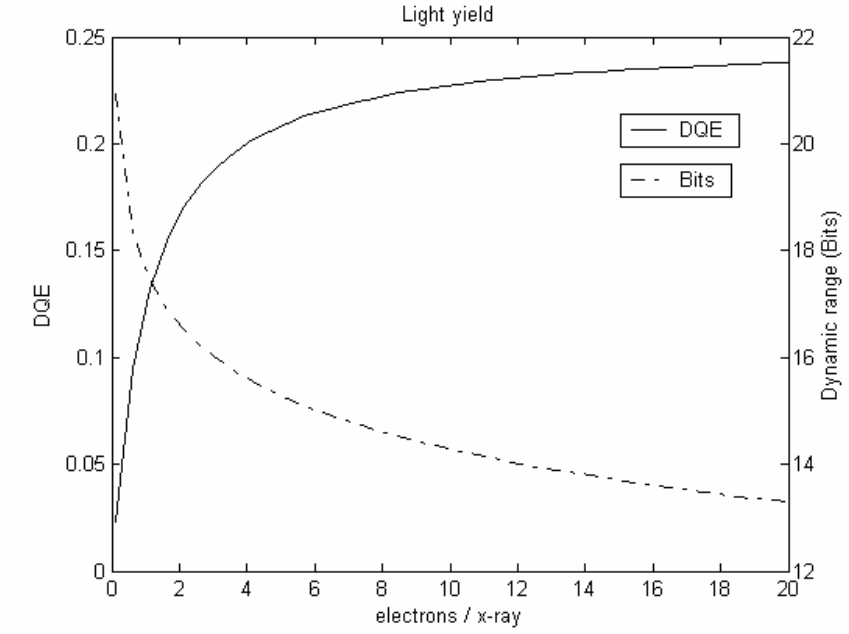

Figure 8. DQE and dynamic range as function of light yield (T_a = 0.25).

8. Lens system

A lens system is used to guide the light from the scintillating screen to the CCD. To protect the CCD from primary radiation it must be placed outside the primary beam. There are two different approaches to be compared; conventional optical lens and fiber optic image conduit.

8.1 Optical lens

An optical lens is the easiest way to guide the light from the scintillating screen to the CCD. The traditional method is to put a 90° mirror in the optical path to move the CCD out of the primary beam. The efficiency of an optical lens coupling, η_{lens}, is given by:

$$\eta_{lens} = T_{lens} / \left[2 f (1 + m^{-1})\right]^2 \tag{5}$$

where, T_{lens} is the transmission of the lens material, f is the f-number of the lens and m is the magnification. As we want a compact system, the lens must have a low f-number which leads to large aberrations. Another implication is the fact that a CCD with large well capacity gives a magnification close to one which means that the spatial resolution at

the edges will be poor with a low f-number. Only lenses with low f-numbers can be used due to the restrictions of the overall length. Even if a lens with higher f-number is used; the distortions are troublesome and the efficiency is far to low.

8.2 Fiber optic image conduit

A fiber optic image conduit or fiber optic lens comprises a ream of glass fibers that is sintered into one solid unit, a multi fiber. It has in principle same properties that single optical fibers. In the case of fiber optic conduit it has to shield the CCD primary x-rays. It can be done either by using material with high attenuation as in the previous version or to bend the fiber optics conduit (see Figure 9). Still having high efficiency and keeping the overall length within the requirements.
The transmission properties should be nearly the same after the bending as before. Macro bending isn't affecting the transmission in single fibers and it should be the same with a fused bundle. If we assume constant volume in the image conduit with 6 µm fibers, the inner fibers will increase diameter from 6 to 6,4 µm and the outer will decrease from 6 to 5,7 µm. The numerical aperture (NA) will change some but it is in the range of what can be compensated with background correction.

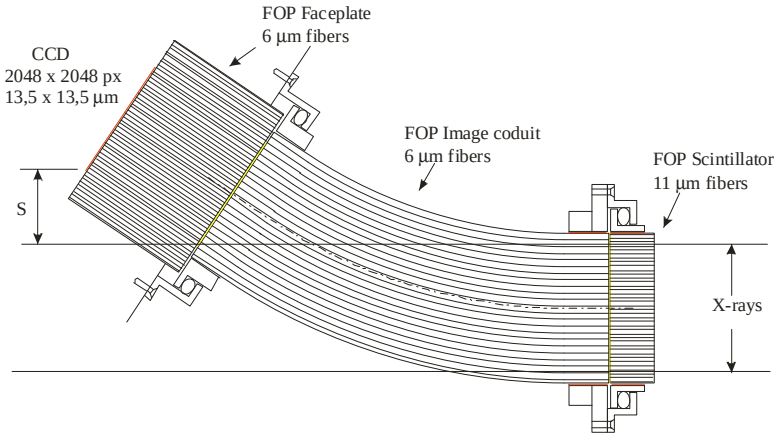

Figure 9. New concept with a bent fiber optic image conduit.

8.3 Radiation induced noise

Experience from the first generation gives that the radiation induced noise produces white dots with about 300 ADU's above the average level. This corresponds to about 15 keV/x-ray detected directly in the CCD which is similar to earlier studies [7]. The intention is to design the x-ray camera in such away that radiation induced noise caused by the primary beam from the x-ray machine will be minimized.
Monte-Carlo simulations show that if the CCD is moved out of the primary beam the radiation induced noise will decrease, which is expected. What is interesting is that when the safety margin, S, (see Figure 9) is more than about 15 mm, the radiation induced noise is completely eliminated. It means that the length of the conduit can be kept within 100 mm.

8.4 Spatial resolution

The resolving power of a fiber optic device is well defined. As a rule, 0.8 photographic line pairs per fiber diameter can be resolved. The resolving power of a system made up of several optical components can be represented as follows;

$$\frac{1}{r_{system}^2} = \frac{1}{r_1^2} + \frac{1}{r_2^2} + \frac{1}{r_3^2} + ... \quad (6)$$

The optical chain in Figure 9, have a fiber optic faceplate as input window coupled in series with the bent image conduit. The system resolution is 25.8 lp/mm and the extra faceplate will decrease the transmission but only lower the resolution slightly. It has been shown (4) that a conversion efficiency of 10-20 light photons / detected x-ray is enough to minimize the SNR. By choosing glass quality of the image conduit and the fiber optic faceplate with proper transmission values it can be tuned together with the FOS-faceplate to achieve the right conversion efficiency.

9. Conclusion

Monte Carlo simulations of the lateral spread of secondary electrons have shown that the energy deposition is very local. By using a FOS-screen that reduces the internal light spread, the spatial resolution can be improved further. The system should also be designed in such way that the conversion efficiency is kept as low as possible without lowering the DQE.
To reduce the radiation induced noise and still keep the overall length to a minimum, the use of a bent fiber optic lens is proposed for the next generation of FOS based x-ray cameras. This will improve the radiographic sensitivity one step further in the field of digital radiography.

References

1. H. Shao, D.W. Miller, C.R Pearsall, Nucl. Instr. and Meth. A299 (1990) p.528
2. L. Hammar, H. Wirdelius, 16th World Conference on Nondestructive Testing, Montreal 2004
3. H. Shao, D.W. Miller, C.R Pearsall, IEEE Trans. Nuc. Sci., NS-38, No. 2, p. 845, 1991
4. R. K. Swank, J. Appl. Phys., Vol. 44, No. 9, September 1973
5. V.V Nagarkar, J.S. Gordon, S. Vasile, , IEEE Trans. Nuc. Sci. NS- 43, No. 3, p.1559, 1996
6. S.M. Gruner, M.W Tate, E.F. Eikenberry, Rev. Sci. Instrum., Vol. 73, No. 8, 2002
7. E.A. Burke, J.J. Boyle, H.J. Huemmler, IEEE Trans. Nuc. Sci., NS-28, No. 6, p. 4068, 1981